J Mol Model (2011) 17:1661–1668
DOI 10.1007/s00894-010-0869-3

ORIGINAL PAPER

Stucture of the complex between *Mucor pusillus* pepsin and the key domain of κ-casein for site-directed mutagenesis: a combined molecular modeling and docking approach

Tiezhu Li · Jinghui Wang · Yuqiu Li · Li Zhang · Li Zheng · Zhuolin Li · Zhennai Yang · Quan Luo

Received: 2 June 2010 / Accepted: 5 October 2010 / Published online: 27 October 2010
© Springer-Verlag 2010

Abstract In the structural-based mutagenesis of *Mucor pusillus* pepsin (MPP), understanding how κ-casein interacts with MPP is a great challenge for us to explore. Chymosin-sensitive peptide is the key domain of κ-casein that regulates milk clotting through the specific proteolytic cleavage of its peptide bond (Phe^{105}-Met^{106}) by MPP to produce insoluble para-κ-casein. Here, we built the model of this large peptide using molecular modeling technique. Docking study showed that MPP can accommodate the designed model with a favorable binding energy and the docked complex has proven to locally resemble the inhibitor-chymosin complex. The catalytic mechanism for the peptide model binding with MPP was explored in terms of substrate-enzyme interaction and property of contacting surface. Some critical amino acid residues in the substrate binding cleft have been identified as an important guide for further site-directed mutagenesis. Glu13 and Leu11 in the S3 region of MPP, predicted as the special mutation sites, were confirmed to retain clotting activity and decrease the proteolytic activity. These novel mutants may provide a promising application for improving cheese flavor.

Keywords κ-casein · Molecular docking · *Mucor pusillus* · Mutagenesis · Secondary proteolysis

Electronic supplementary material The online version of this article (doi:10.1007/s00894-010-0869-3) contains supplementary material, which is available to authorized users.

T. Li · J. Wang · Y. Li · L. Zhang · L. Zheng · Z. Li · Z. Yang
Center of Agro-food Technology,
Northeast Agricultural Research Center of China,
No. 1363 Cai-Yu Street,
Changchun, Jilin Province 130033, People's Republic of China

L. Zhang · L. Zheng · Z. Yang (✉)
College of Biological and Agricultural Engineering,
Jilin University,
Changchun 130025, People's Republic of China
e-mail: zyang@cjaas.com

Q. Luo (✉)
State Key Laboratory of Theoretical and Computational Chemistry, Institute of Theoretical Chemistry, Jilin University,
Changchun 130023, People's Republic of China
e-mail: luoquan@jlu.edu.cn

Introduction

Chymosin extracted from the abomasum of unweaned calves has traditionally been used as a milk clotting agent for cheese manufacturing [1, 2]. Since 1990, the application of bovine chymosin in the dairy industry was diminishing with a global shortage of calves. Microbial rennin is replacing bovine chymosin, because more than half of the world's cheese production is based on microbial rennet. Among a number of rennet substitutes, *Mucor pusillus (M. pusillus)* and *Mucor miehei* pepsin as the representative fungal enzymes have attracted much attention. Both enzymes have the same milk clotting activity as bovine chymosin and can specifically cleave the chymosin-sensitive Phe^{105}-Met^{106} linkage of κ-casein to produce insoluble para-κ-casein, which causes casein micelles to aggregate and form a clot. Compared with bovine chymosin, however, Mucor rennins possess the lower proteolytic specificity but the higher thermostability [3–5]. Using these enzymes to produce cheese, its hydrolysis activity is retained after blanching treatment, and the residual milk clotting enzymes in curd could further catalyze the proteolysis of para-κ-casein during cheese ripening, resulting in a bitter and soft product [6].

To improve the milk clotting characteristics of Mucor rennin for commercial use, considerable effort is devoted to

generating the artificially mutated enzymes with improved properties [7]. For example, Branner and coworkers reported that chemical modification of Mucor rennin had been established to reduce its heat resistance [8]. Recently, Yamashita and Hiramatsu's group reported that the heterologous expression secretion system of the *M. pusillus* rennin gene in Saccharomyces cerevisiae is expected to be useful for mutagenesis of MPP [9–11]. Despite some progress made in the past years, the search for novel Mucor rennin mutants has so far been limited due to the lack of information on the structural basis of the interaction between Mucor rennin and κ-casein, because the X-ray structure of κ-casein is not available yet. Thus, exploring the local structure of the peptide surrounding the chymosin-sensitive Phe^{105}-Met^{106} linkage, investigating the mechanism of this peptide interacting with Mucor rennin, and developing novel mutants of Mucor rennin with low secondary proteolytic activity are of great interest to us.

In this study, we presented the appropriate model of the chymosin splitting domain (CSD, Peptide His^{102} Leu^{103} Ser^{104} Phe^{105} Met^{106} Ala^{107} Ile^{108}) in κ-casein based on the similarities that this peptide could share with other proteins of known three-dimensional structures. Ligand docking starting from this peptide model complexed with MPP enables us to predict its binding mode. Some critical residues involved in ligand binding have been identified according to the structure of the docked complex, and it plays a key role in the design of novel mutants that have a practical value for promoting the flavor of cheese. The simulation result has assured our site-directed mutagenesis can be accurately introduced into the wild-type MPP to yield two mutants, which were confirmed to cause a decrease in secondary proteolysis.

Theory and methods

To ensure that CSD had a reasonable conformation and orientation, its templates were selected not only for high sequence similarity, but also for consistent secondary structure. The sequence of chymosin-sensitive linkage (CSL, amino acid from Met95 to Lys116) in κ-casein was extracted to carry out the local similarity searches using PSI-BLAST and PHI-BLAST [12]. Several programs involving PROF [13], SSPRO [14], YASPIN [15], PSIPRED [16] and SYMPRED [17] were used to analyze the secondary structural feature of κ-casein. Based on the provided template structure, the three-dimensional (3D) model of CSD was built and refined via three steps by using Insight II software [18]. First, the backbone coordinates of CSD were copied from the template protein, and each side chain in the template was replaced by that of the corresponding target residue by aligning the Cα-Cβ bond. Second, Auto_Rotamer in Homology module was employed to adjust the conformation of each side chain. Finally, the CSD model was minimized to a convergence criterion. The quality of the refined CSD model was subsequently checked by comparing the conformation of CSD with the inhibitor in chymosin.

The final CSD model was docked into the X-ray crystal structure of MPP (PDB ID: 1MPP, available from the RCSB Protein Data Bank) [19] to study its binding mechanism. All calculations were performed on Linux Red Hat platform using the Affinity module of Insight II. To consider the solvent effect, the centered enzyme-substrate complex was solvated in a sphere of TIP3P water molecules with radius 5 Å, and the potential functions were set up using the consistent-valence force field (CVFF). We first defined a binding site subset by superimposing the structure of chymosin-inhibitor complex onto MPP. These atoms involving the interacting residues, water molecules, and substrate in the binding site were considered to be movable during the course of docking calculation. Then, a two-step docking procedure was implemented to dock CSD into MPP's binding site by using a fully flexible molecular docking algorithm that combines Monte Carlo, simulated annealing, and minimization. During the first phase, the Monte Carlo minimization approach was used to obtain reasonably placed ligands, and the Quartic-Vdw-no-Coul nonbond method was used for nonbond contacts. By using the initial structures generated by the first phase of the Monte Carlo minimization, we implemented a more realistic approach, the cell-multipole nonbond method, to further refine the docking result [20]. Finally, a set of complex structures was generated and the best structure was selected from them by analysis of interaction energy terms, intramolecular and intermolecular interactions, buried surface area, and stereochemical quality [21, 22].

The docking result is an important guide to design of MPP's mutants. We carried out Site-directed mutagenesis based on the docked complex structure, using the method of Kunkel [23] with the following oligonucleotides: GACTTTGACAGGGAGGAGTAC (L11R); GACTTG GAGCCGTACGCCATT (E13P); ACCGGCAC CAGCCTTCTTCAT (N219S). MPP and its mutants were produced and purified in the same way as described by Zhang et al. [24]. Briefly, plasmid pPICZaA/Mur and its derivatives, in which the MPP gene was placed under the control of the AOX1 promoter, were constructed in E. coli Mur and introduced into Pichia pastorisGS115. MPPs were purified to homogeneity from culture media of yeast using a series of column chromatographies.

The clotting activity was measured by the method of Norma FIL-IDF 110A using 100 μl proteinase solution [25]. The assay mixture including 10 ml standardized milk

and 100 μl of 1 M CaCl2 was incubated at 35 °C for 5 min. The reaction was started by adding the enzyme solution, and the clotting activity was determined by measuring milk-clotting time. One unit of clotting activity was defined as the amount of enzyme that coagulates 1 ml of milk in 40 min, while the result is the average of three samples.

The proteolytic activity was analyzed according to the description by Chitpinityol et al. [26]. The reaction mixes, 20 μl of proteinase solution and 200 μl of 2% acid-denatured haemoglobin, was added to each of the tubes. After 10 min of incubation at 37 °C, the reaction was stopped by the addition of 400 μl of 5% trichloroacetic acid. The mixture was then centrifuged for 10 min at 6500 rpm to collect the supernatant. Absorption at 280 nm was measured, and the result is the average of three samples.

Results and discussion

Because there is no overall sequence homology between κ-casein and other proteins with known structure, we first focused on the alignment of CSL of κ-casein against the PDB database. The PSI-BLAST and PHI-BLAST search based on the local sequence in this region resulted in several homologous protein fragments, which exhibited differences in its secondary structures. We then performed further sorting by selecting sequences for which the observed secondary structures matched the predicted secondary structure of κ-casein. According to the results analyzed by all the secondary structure prediction programs, that the secondary structure surrounding Phe^{105}-Met^{106} in κ-casein is a β-strand (Fig. 1a), we finally selected two fragments, glutamine synthetase (PDB ID: 2GLS) [27] and ornithine carbamoyltransferase (PDB ID: 1DXH), as templates to build the CSD model. Figure 1a shows the common β-strand conformation of the two peptide fragments with the corresponding sequences aligned with CSL, and the coordinates of the residues in this region were copied from these templates to generate the initial model of CSD. Energy minimization was performed with the criterion that the maximum force of the whole system should be below 10.0 kcal (mol Å)$^{-1}$, to optimize the poor steric contacts. Generally, the substrate can adopt a similar conformation to those found in other enzyme-inhibitor complexes. Interestingly, the refined CSD model fits well with the extended β-strand observed for the chymosin reduced bond inhibitor CP-113972. As shown in Fig. 1b, the side chains of Phe^{105} and Met^{106} in the substrate is orientated similarly to the cyclohexyl ring and propyl group of CP-113972, suggesting that the predicted CSD model is reasonable and can be hydrolyzed by MPP with a similar catalytic mechanism to chymosin. On the other side of the scissile bond (Phe^{105}-Met^{106} peptide bond), His^{102} and Leu^{103} side chains display large shifts relative to the phenol and pyrrole group of CP-113972. This conformational analysis indicates that some changes would occur in the proteolytic specificity of MPP.

To define the substrate binding pocket for MPP, the coordinates of the backbone Cα atoms of MPP and chymosin (PDB ID: 1CZI) [28] were superimposed using Pymol program. The ligand CP-113972 is kept inside the active site of chymosin during the superposition process. As shown in Fig. 2, the active site of MPP is well superimposed on that of chymosin, where inhibitor CP-113972 is bound. However, the superposition reveals that the substrate binding cleft of MPP is different from that observed in chymosin, especially around the phenol and pyrrole group of CP-113972. The surface of the putative pocket in MPP has a serious conflict with the groups mentioned above, indicating that residue substitution

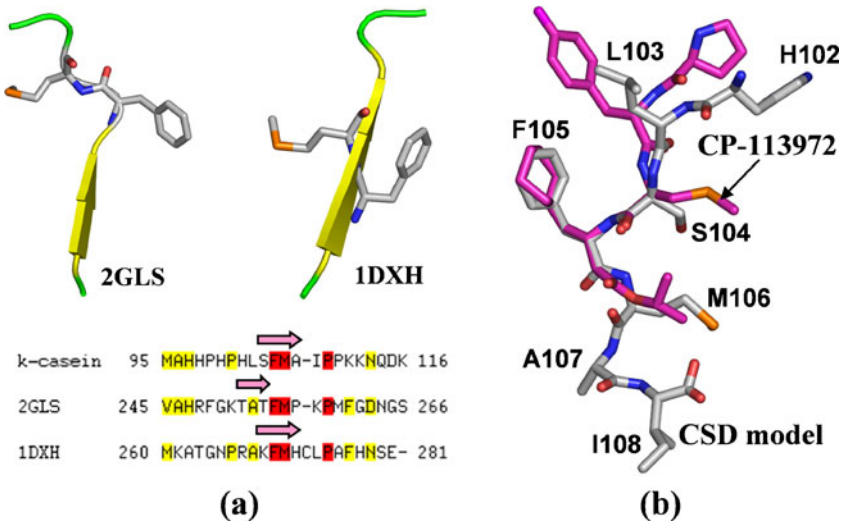

Fig. 1 (**a**) The X-ray structure of two template fragments, 2GLS and 1DXH, and sequence similarities relative to the κ-casein based on the multiple sequence alignment results. The red and yellow boxes represent identical residues and conserved substitutions respectively. The secondary structure prediction results of the κ-casein sequence were obtained using PROF, SSPRO, YASPIN, PSIPRED, and SYMPRED tools. The consensus β-strand motifs are shown with a magenta arrow up to its sequence. (**b**) Comparison of the refined CSD model with chymosin's inhibitor CP-113972

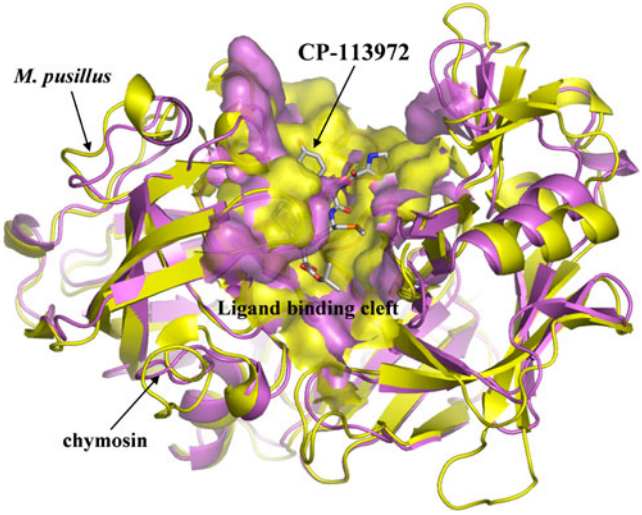

Fig. 2 The binding pocket for MPP defined by superimposing its structure onto that of chymosin with ligand CP-113972 engulged

surrounds the phenol and pyrrole group could affect its substrate specificity.

The docking study was subsequently carried out to investigate the specific binding of CSD to MPP. Results reveal that the most important residues for binding are highly conserved with respect to MPP, and it can accommodate the designed CSD model with the total interaction energy (E_{total}) of -182.42 kcal mol^{-1}, van-der-Waals energy (E_{vdw}) of -94.24 kcal mol^{-1}, and electrostatic energy (E_{ele}) of -99.18 kcal mol^{-1}. Figure 3a,b shows the interface between CSD model and MPP. Residues involved in substrate binding are shown in Fig. 3c. The active site cleft is apparently formed by several β-strands, which contain the catalytic aspartate residues (Asp32 and Asp215 in S1 region) conserved in all known chymosin [29]. The side chain of Asp32 can form a hydrogen bond with the carbonyl oxygen of CSD, while Asp215 tightly bound one water molecule is proposed to nucleophilically attack the Phe^{105}-Met^{106} peptide bond carbonyl to form a tetrahedral intermediate. Earlier mechanism has assumed that the oxyanion of the intermediate is stabilized by the hydrogen bonds with the NH group of Gly76 and possibly of Thr77 [30]. In our docked complex model (Fig. 4a), however, the oxyanion is stabilized by hydrogen bonds to the negatively charged carboxyl of Asp32. Gly76 and Gly217 can form hydrogen bonds with the peptide CO and NH of CSD to maintain a suitable conformation of substrate for initiating the nucleophilic attack. Herein, the catalytic mechanism for MPP based on this docked structure is proposed (Fig. 4b). The reaction is believed to occur in two steps: I) The water molecule polarized by Asp215 can nucleophilically attack the scissile bond carbonyl group to form the tetrahedral intermediate, while a proton transfer from Asp32 to the carbonyl oxygen of substrate. The transition state is subsequently stabilized by a negative charge localized on the deprotonated Asp32. II) The product is formed by specifically cleaving the scissile C-N bond between Phe^{105} and Met^{106}. This process is accompanied by the transfer of two protons. One is from the Asp215 to the leaving amino group of Met^{106}, and the other is from water molecule to Asp32.

In addition to these conserved catalytic residues presented above, residue substitutions occurred in the substrate binding cleft in the region of P3, P2, P1, S1, S2, S3, and S4 would make a major contribution to the substrate specificity for MPP. Comparing MPP's three-dimensional structure with chymosin shows that MPP exhibits an apparent difference around the P3 region (Fig. 5). Several insertions were found in a large loop and α-helix in this region, including residues: Asp183 to Trp190 and Pro126 to Phe151. Computational results shown that the guanidine group of Arg186 is able to make a strong electrostatic interaction with the negative carboxyl of Ile^{108}, with the corresponding electrostatic energy of -19.20 kcal mol^{-1}. Residues Phe188 and Phe189 are another pair of interesting residues in this loop. The benzene rings in Phe188 and Phe189 cause favorable interactions with Ile^{108} because the calculated total interaction energy between two phenylalanine and CSD is -6.35 and -6.40 kcal mol^{-1}, respectively. Furthermore, the NH of Asn128 can form a hydrogen bond with the NH of Ile^{108} and the guanidine of Arg186 interacts with the carboxyl of Ile^{108} via multiple hydrogen bonds. Ala131 makes close contact with the sec-butyl group of Ile^{108}. These interactions could have contributed to the high binding affinity of CSD for MPP.

For the second region P2, we observed a relatively small number of contacts. Gly34 is hydrogen bonded to the NH of Ala^{107}, and the binding contact is further reinforced with the interactions between the side chain of Ala^{107} and Ser35; Asn128 and Phe189. Residues surrounding Gly34 were structural aligned in MPP to the corresponding region of chymosin. Due to a high homology between MPP and chymosin structure in this region (Fig. 5), it is likely that Ala^{107} of κ-casein is placed in a topologically similar position to that of the residue in chymosin.

As mentioned above, Phe^{105}-Met^{106} peptide bond is sensitive for enzymatic cleavage. This can be explained by the observation during docking simulation. The conformation of CSD is found to be strongly induced by the shape of the MPP binding channel which forces Phe^{105}-Met^{106} peptide backbones to adopt a tighter conformation, compared to that of the free state. As shown in Fig. 3, the loop located in the P1 and S1 region, known as the β-hairpin "flap" in chymosin, can move a lot to cover and accommodate the benzene ring of Phe^{105}. Tyr75, an absolutely conserved residue, is present near the tip of the flap and is proven to be a crucial residue in the capture of the substrate, as the

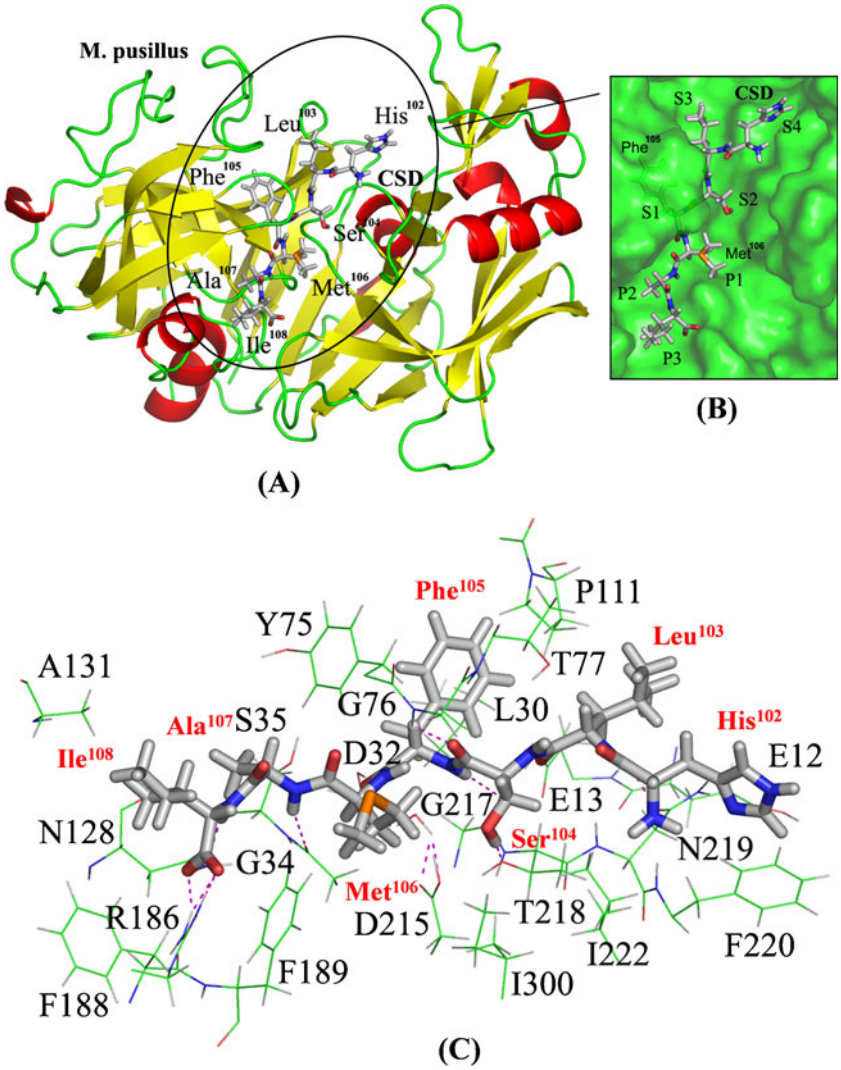

Fig. 3 (**a**) The docked structure of CSD-MPP complex. (**b**) The solvent accessible surface of the active site cleft for MPP. The scissile peptide bond is buried within the enzyme S1 pocket, which provides a tight packing around Phe[105] and Met[106] of CSD. (**c**) The detailed interaction mode between CSD and MPP. Hydrogen bonds are represented by magenta dotted lines

calculated total interaction energy of this residue with the substrate is -15.49 kcal mol^{-1}. This interaction energy analysis also found that the specific ring stacking interaction is the major force that stabilizes the benzene ring of Phe[105] (E_{vdw} and E_{ele} are -11.65 and -3.84 kcal mol^{-1}, respectively). This result is consistent with previous experimental data for *Rhizomucor pusillus* pepsin where weak activity was observed in Tyr75Phe, and other mutants excluding asparagine showed significantly decreased or negligible activity [31]. Moreover, Gly217 participates in binding contacts by creating a hydrogen bond with the main chain NH group of Phe[105]. Residues Leu30, Thr77, Pro111, and Ile120 are able to make an additional contact with the substrate because its side chains can provide a considerable hydrophobic environment for the benzene ring of Phe[105]. The corresponding interaction energy between CSD and each residue mentioned above is calculated to be higher than -4.00 kcal mol^{-1}, which indicates that these hydrophobic contacts could slightly increase the affinity of the substrate. In contrast to the hydrophobic environment of the S1 region, the P1 region is partially solvent-exposed to ensure that the water molecules could enter the catalytic center. Several residues involving Thr213, Ile300, Phe189, Gly76, and Tyr75 are bound with Met[106] to assist in keeping a suitable conformation of the scissile peptide bond for the nucleophilic attack. These residues are relatively conserved, only Phe189 and Thr213 are replaced with Tyr189 and Ile213 in chymosin.

On the other side of the scissile Phe[105]-Met[106] peptide bond, CSD is stabilized by making a number of contacts with S2, S3, and S4 region. In addition to Gly76, which had been previously shown to be important to the S2 region, Thr218 is able to form a hydrogen bond with the hydroxyl group of Ser[104]. This residue is evolutionarily conserved throughout all chymosin, implicating the significant function of S2 region in the stabilization of Ser[104].

Next, we analyzed other two regions for specific substrate recognition. As described above, MPP has an apparently different structure from chymosin at the S3 and S4 region. Sequence alignment shows that residues in these regions are highly variable. As shown in Fig. 6, residue 13

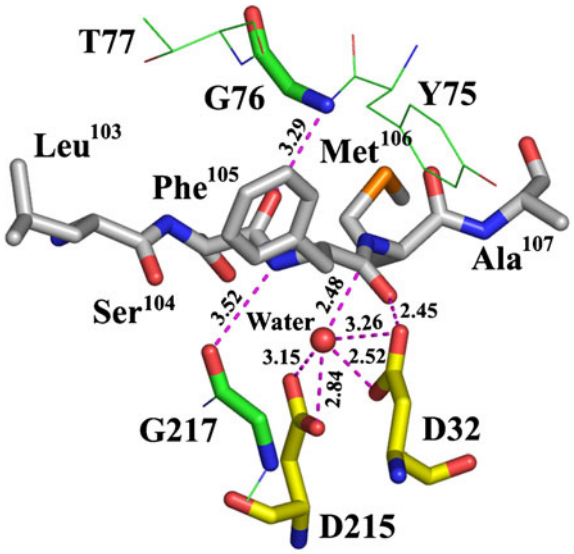

(A)

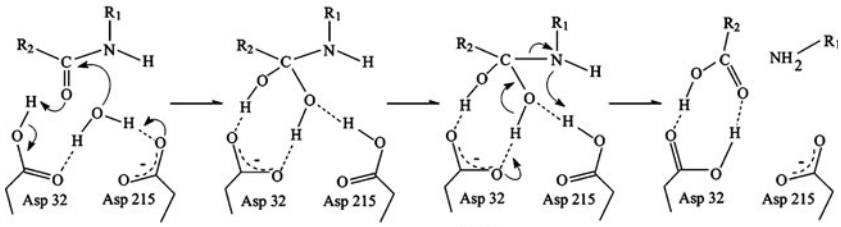

(B)

Fig. 4 (**a**) Close-up view of CSD in the catalytic center of MPP obtained in the docking calculations. Water molecule situated between the active aspartates Asp32 and Asp215, in combination with highly conserved Tyr75 and Gly76, are shown. The distances are marked in magenta dotted lines. (Unit: Å). (**b**) Catalytic mechanism for MPP proposed in this work

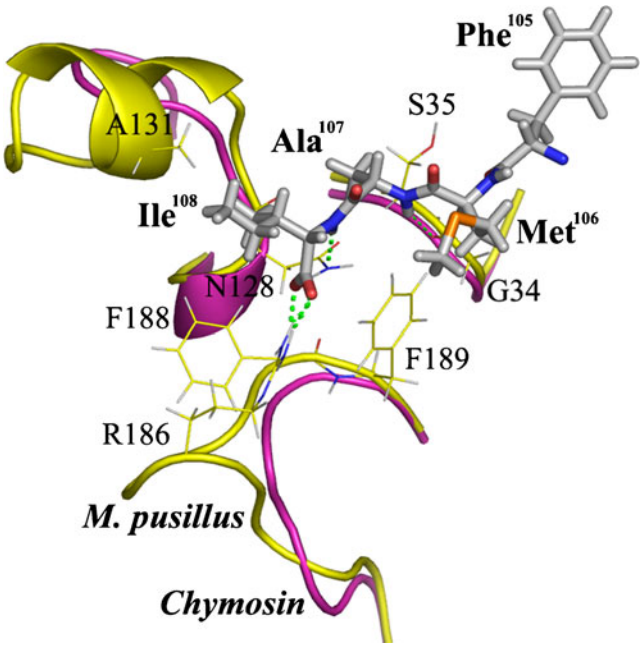

Fig. 5 Superposition of the chymosin crystal structure (magenta) with the docked CSD-MPP complex structure (yellow), showing a significant difference in P3 region

in chymosin is Gln, whereas it is replaced by Glu13 in MPP. The conformational difference between Glu and Gln in that position is apparent on its side chains, which flank both side of *Loop I*, with the former sharing a closer interaction with Leu^{103} of CSD than the latter. Residues Ser12 and Asp11 of chymosin were also replaced by Glu12 and Leu11. The two substitutions in MPP are sufficient in altering the conformation of *Loop I*, leading to a sharp bend of the structure relative to that in chymosin. Obviously, the bend observed in MPP allows for additional contact of CSD with *Loop I*, in which Leu11 provides a hydrophobic binding region to stabilize the side chain of Leu^{103}. Furthermore, P111, rather than Leu111, in the *Loop III* was observed to approach Leu^{103} to reinforce the hydrophobic interaction. The substitution of Ser219 for Asn219 can introduce a hydrogen bond between the amide group of Asn219 and the NH of Leu^{103}. These evolutionary differentiations in the S3 region might be responsible for the proteolytic specificity of MPP.

For the S4 region, the docking results highlight the binding of CSD with *Loop II*. Although *Loop II* in MPP and chymosin adopt a highly similar conformation, the Asn/Ser-219 and Phe/Lys-220 changes that occurred in this loop of MPP not only causes an increase in the hydrogen bond between the amide group of Asn219 and the amino

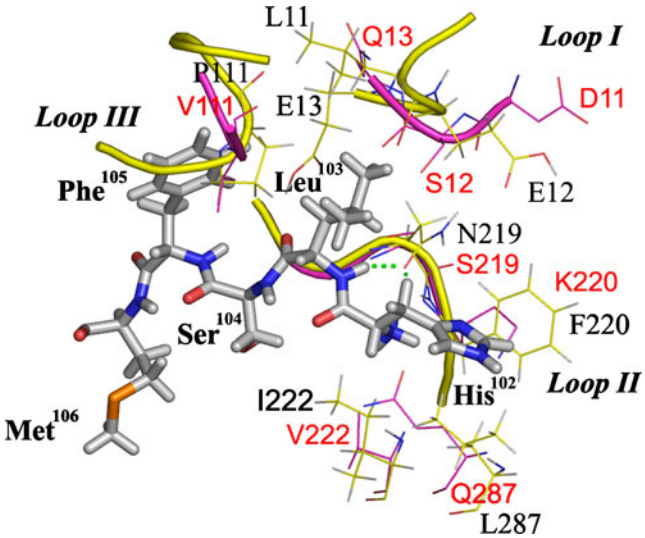

Fig. 6 Comparison of the S3 and S4 region of MPP (yellow) with chymosin (magenta). Some significant residue substitutions are presented in these variable regions. Hydrogen bonds are represented by green dotted lines

group of His[102], but also introduces a strong van-der-Waals (vdw) attractive force between the phenyl ring of Phe220 and the pyrrole group of His[102]. In addition, Gln287 and Val222 were replaced by Leu287 and Ile222 to provide a more comfortable hydrophobic environment for His[102]. These favorable residue substitutions may play an important role in the proteolytic specificity of MPP.

To further elucidate the structural roles of the substituted amino acid residues, a quantitative energy calculation was carried out between CSD and each residue in S3 and S4 region to investigate its energy contributions. Table 1 lists the detailed interaction energy including total interaction energy, van-der-Waals energy, and electrostatic energy. The computational results presented here are consistent with the previous structural analysis. Asn219, with the highest binding affinity, appears to be a crucial residue in stabilizing the main chain of Leu[102] and His[102]; possesses the lowest total interaction energy: -17.75 kcal mol^{-1}. The residue with the second lowest interaction energy is Glu13, with a value of -5.30 kcal mol^{-1}. Next are Leu11, Glu12, and Pro111- with interaction energies of -3.63, -3.52, and -3.48 kcal mol^{-1}, respectively. Phe220, Leu287, and Ile222 have the highest interaction energy, which are all more than -1.80 kcal mol^{-1}. Because the interaction energy analysis indicates the ability of the previously mentioned residues to bind with CSD for substrate recognition, Asn219, Glu13, and Leu11, with the lowest interaction energy, appear to be suitable locations for site-directed mutagenesis to change the proteolytic activity.

In order to test this hypothesis, we constructed several mutants at position 11, 13, and 219 to examine its clotting and proteolytic activities. Interestingly, all the predicted mutants including Leu11Arg, Glu13Pro, and Asn219Ser retained clotting activity and changed the proteolytic activity to some degree. Our experimental results show that the proteolytic activity of non-mutated MPP is 19.50 U/ml, while the proteolytic activity of mutants Leu11Arg, Glu13Pro, and Asn219Ser are 19.35, 16.25, and 20.02 U/ml, respectively. One explanation for this phenomenon is that these residue substitutions are far from the reactive center, which causes a neglectable effect on the nucleophilically attack in changing the clotting activity. Mutating position 11 to Arg could damage the proper hydrophobic environment of the S3 region, leading to a slight decrease in proteolytic activity. Consistent with position 11, introduction of the Pro residue into position 13 causes an apparent decrease in proteolytic activity. This indicates that the direct electrostatic interaction of Glu13 with the main chain of CSD is an important factor for enhancing the proteolytic activity. As for position 219, the loss of the hydrogen bonds created by the Asn219Ser mutation could cause an unfavorable interaction of CSD with the binding pocket at the S3 and S4 region, which was expected to result in a large loss of proteolytic activity. However, mutation result failed to show a decrease in proteolytic activity. This implies that the truncated κ-casein would affect the structure at the end of the CSD model, where the conformation of His[102] is more flexible than that in the intergrated κ-casein.

The ratio of clotting activity to proteolytic activity (C/P) is a key parameter for MPP to improve cheese flavor [32]. Experimental results show that the clotting activity did not

Table 1 The interaction energy between substrate CSD and each residue in S3 and S4 region

Residue	E_{vdw} (kcal mol^{-1})	E_{ele} (kcal mol^{-1})	E_{total} (kcal mol^{-1})
Leu11	-1.72	-1.91	-3.63
Glu12	-0.73	-2.79	-3.52
Glu13	-3.86	-1.44	-5.30
Pro111	-4.23	0.75	-3.48
Asn219	-4.06	-13.69	-17.75
Phe220	-5.35	3.62	-1.73
Ile222	-2.04	1.37	-0.67
Leu287	-3.44	2.19	-1.25

change in mutated and non-mutated MPP, which is 63.38± 0.05 U/ml. This means that the invariable clotting activity combined with the decreased proteolytic activity can assure a high yield of curd without extensive proteolysis to affect the flavor of cheese. Thus, it should be noted that Glu13Pro and Leu11Arg mutants show an increase in the C/P ratio without a significant loss in clotting activity, indicating that the mutated MPP has practical value in the cheese industry.

Conclusions

Based on the template of the two fragments from 2GLS and 1DXH, we have built the model for the key domain (CSD) of κ-casein to study the detailed binding mechanism of κ-casein with MPP. The refined CSD model closely resembles the inhibitor of chymosin surrounding the scissile Phe-Met bond and can be fitted well with the MPP's substrate binding cleft with a high affinity. Based on the ligand docking analysis, a number of residues that contact the ligand have been identified. We proposed a different mechanism from the one accepted, in which the oxyanion of the reactive intermediate is stabilized by Gly76 rather than Asp32. Structural analysis, combined with interaction energy results, enable us to pinpoint several amino acid residues including Asn219, Glu13, and Leu11- which are believed to be suitable sites for site-directed mutagenesis to change the proteolytic activity. Among the mutants constructed, Glu13Pro and Leu11Arg mutants were confirmed to increase the ratio of clotting activity to proteolytic activity without a significant loss of clotting activity. These novel mutants may be promising candidates for milk coagulant to produce cheese with good flavor.

Acknowledgments This work was supported by National 863 Program 2006AA10Z306, National Public Benefit Research (Agriculture) Foundation (200903043), China Postdoctoral Science Foundation funded project (20100471246), Natural Science Foundation of China (31071574), Natural Science Foundation for the Youth (21004028) and The Earmarked Fund for Modern Agro-industrial Technology Research Systems in China (Nycytx-05-02).

References

1. Beppu T (1983) Trends Biotechnol 1:85–89
2. Foltman B (1966) CR Trav Lab Carlsberg 35:143–231
3. Drøhse HB, Foltmann B (1989) Biochim Biophys Acta 995:221–224
4. Martin P, Raymond MN, Bricas E, Dumas BR (1980) Biochim Biophys Acta 612:410–420
5. Jollès P, Alais C, Jollès J (1963) Biochim Biophys Acta 69:511–517
6. Egitoa AS, Girardetc JM, Lagunaa LE, Poirsonc C, Molléb D, Micloc L, Humbertc G, Gaillardc JL (2007) Int Dairy J 17:816–825
7. Yamashita T, Higashi S, Higashi T, Machida H, Iwasaki S, Nishiyama M, Beppu T (1994) J Biotechnol 32:17–28
8. Branner-Jørgensen S, Eigtved P, Schneider P (1981) Neth Milk Dairy J 35:361–364
9. Yamashita T, Tonouchi N, Uozumi T, Beppu T (1987) Mol Gen Genet 210:462–467
10. Hiramatsu R, Aikawa J, Horinouchi S, Beppu T (1989) J Biol Chem 264:16862–16866
11. Hiramatsu R, Yamashita T, Aikawa J, Horinouchi S, Beppu T (1990) Appl Environ Microbiol 56:2125–2132
12. Altschul SF, Madden TL, Schäffer AA, Zhang J, Zhang Z, Miller W, Lipman DJ (1997) Nucleic Acids Res 25:3389–3402
13. Ouali M, King RD (2000) Protein Sci 9:1162–1176
14. Pollastri G, Baldi P (2002) Bioinformatics 18(Suppl 1):S62–S70
15. Lin K, Simossis VA, Taylor WR, Heringa J (2005) Bioinformatics 21:152–159
16. Jones DT (1999) J Mol Biol 292:195–202
17. Simossis VA, Heringa J (2004) Bioinformatics (in press)
18. InsightII, Homology User Guide, SanDiego:Biosym/MSI (2000)
19. Newman M, Watson F, Roychowdhury P, Jones H, Badasso M, Cleasby A, Wood SP, Tickle IJ, Blundell TL (1993) J Mol Biol 230:260–283
20. Affinity San Diego Molecular Simulations Inc (2000)
21. Bartlett PA, Shea GT, Telfer SJ, Waterman S (1989) R Soc Chem 182–196
22. Shoichet BK, Kuntz ID, Bodian DL (1992) J Comput Chem 13:380–397
23. Kunkel TA (1985) Proc Natl Acad Sci USA 82:488–492
24. Zhang J, Zhang SQ, Wu X, Chen YQ, Diao ZY (2006) Process Biochem 41:251–256
25. International Dairy Federation: Brussels, Belgium (1987) Calf rennet and adult bovine rennet:Determination of chymosin and bovine pepsin contents (chromatographic method). Standard 110A
26. Chitpinityol S, Goode D, Crabbe MJC (1998) Food Chem 62:133–139
27. Yamashita MM, Almassy RJ, Janson CA, Cascio D, Eisenberg D (1989) J Biol Chem 264:17681–17690
28. Groves MR, Dhanaraj V, Badasso M, Nugent P, Pitts JE, Hoover DJ, Blundell TL (1998) Protein Eng 11:833–840
29. Chitpinityol S, Crabbe MJC (1998) Food Chem 61:395–418
30. Pearl LH (1987) FEBS Lett 214:8–12
31. Park YN, Aikawa J, Nishiyama M, Horinouchi S, Beppu T (1996) Protein Eng 9:869–875
32. Aikawa J, Yamashita T, Nishiyama M, Horinouchi S, Beppu T (1990) J Biol Chem 265:13955–13959